

STUDY ON THE INFLUENCE OF THE CONFINEMENT EFFECT ON THE BOND STRENGTH RECOVERY IN THE DEFECTIVE GROUTED SLEEVE CONNECTION

Kulondwa Kahama Espoir, Xie Fuzhe, Ali Abdulkadir Aden and Faisal Iliasu Illo

Jiangsu University, Faculty of Civil Engineering and Mechanics, Department of Civil Engineering, Zhenjiang, 301 Xuefu road, China; espoirkulondwa@gmail.com, xiefuzhe@ujs.edu.cn, calidhuux88@outlook.com

ABSTRACT

Defects emanating from the onsite operation of the grouted sleeve connector have a significant impact on the ultimate tensile capacity of the connector. In this research, an experiment on the capacity of the fully grouted sleeve connector considering different configurations of defects was carried out. The experiment results indicated that the connector is highly sensitive to the location of the defects, which engenders a drop of 15% in the ultimate capacity of the connector. Based on the accurate simulation of the experiment model, a series of parametric analyses were conducted to evaluate the interaction of defects with other mechanical properties of the connector. It was found that the different values of the ratio of the sleeve diameter to that of the bar within the design recommended interval significantly influence the connection's performance. The lowest ratio value engenders approximately 10% to 16% of tensile strength recovery in the weakened configuration, while a bigger ratio value engenders a decline in the capacity. This work proposes the incorporation of a safety constant in the average bond expression.

KEYWORDS

Bond strength, Grouting defect, Confinement effect, Interfacial modeling, Grouted sleeve connection

INTRODUCTION

Grouted sleeve connections are one of the frequent ways of connecting precast concrete components in the construction industry [1]. This kind of connection is achieved by the confinement of high-strength, non-shrink grouting materials in the sleeve splice where two reinforcements are connected. Given the relevance of connections in the structural integrity of precast concrete members, various research avenues were undertaken to confirm the reliability of this connection.

Early investigations on the grouted sleeve connector focused on its mechanical properties by subjecting the connector to a tensile loading test [2-4]. It is found that an adequate integration of each of the mechanical properties can sustain the tensile performance of the connector up to the fracture of the bar. This indicates that the connector can achieve and outperform the tensile

resistance of the reinforcement bar [2, 4, 5]. The mechanical properties of the connector are mainly influenced by the embedded length of the rebars, the bond strength, and the diameter of the iron sleeve.

In the quest of expanding research on the reliability of the grouted sleeve connection, studies combined experimental and theoretical approaches to assessing the earthquake performance of the connector [6-9]. It was found that the connector's performance largely depends on a good configuration of its mechanical properties and mainly the bond [10].

Studies on the bond between the bar and the grouting materials have confirmed a strong relationship between the bond strength and the anchorage length [11-15]. In the grouted sleeve connector, the bond strength is the main component of resistance when the connector is subjected to loading [14, 16, 17]. Experimental research on the connector revealed that the mechanical interlocks developed by the deformed bar largely contribute to the bond formulation. At the same time, good chemical adhesion and the high compressive strength of the grouting materials are important characteristics and result in additional enhancement of the bond performance [18].

However, during the onsite grouting process, sometimes an error resulting from the manipulation of the grout inlet or outlet hinges and the manual preparation of grouting materials causes defects within the sleeve. Currently, research interests on grouted sleeves focus on the influence of the defects on the connector's performance.

The investigations on defective grouted sleeve connectors found that the presence of defects within the connector can significantly reduce the tensile and seismic resistance of the connector. Xu uniformly mixed soil and foaming agents as defects in grouting material during his experimental research and found that 30% of defects in the total mixture significantly reduced the bond performance and precipitated the failure of the connector [19]. Most recently, Zheng presumed the defects reduced the bar's embedded length and subjected the defective connector to tensile and cyclic loading. He found that when the embedded length is $4d$ the tensile performance is compromised, while during the cyclic resistance was compromised when the anchorage length was equal to $5d$, where d is the diameter of the bar [20]. Further investigations of defects within the connector used a similar approach of predesigned defects to assess the connector's performance. They confirmed that defects significantly weaken the resistance of the connection even in a post-fire analysis completed by Zhang [5, 21]. However, most of these studies concentrated more on a half-grouted sleeve than a fully grouted sleeve. They either relate embedded length reduction defects and distributed defects to the tensile performance and seldom consider the influence of the location of the defect on the performance of the connector.

Further research on the bond performance of the connector found that the confinement pressure from the sleeve impacts the bond performance [12, 22, 23]. The impact of the confinement effect within the sleeve can vary based on the ratio of the sleeve diameter to that of the reinforcement bar [24, 25]. In summary, provided by Espoir K in his theoretical research, the bond performance of the connector has an inverse proportionality with the sleeve diameter [26, 27]. A comprehensive analysis of the impact of defects requires additional investigation on how the defects interact with the change in the mechanical properties of the connector.

This paper analyses the impact of the confinement effect resulting from the diameter of the sleeve on the bond strength degradation and recovery of a grouted sleeve connection predesigned with defects and the induced consequences on the tensile performance of the connector. This article further studies the influence of the positioning of the defects in interaction with the possible degrees of confinement of grouting materials within the sleeve through a

parametric analysis. The findings of this research aim to enlighten the structural health monitoring process of the defective grouted connection and to propose an optimized configuration for the components of the grouted sleeve connection

THE EXPERIMENT OF FULLY GROUTED SLEEVE CONNECTOR

Material's properties and material's model

The materials properties of the bar are drawn from the tensile experiment of a steel bar used in the experiment of this work. The diameter of the bar in the experiment was constant at 14mm but changed in the proposed parametric study. The materials properties of the bar are listed in Tab. 1.

Tab. 1 - Material model of the reinforcement bar

Material density (kg/m ³)	Yield strength (MPa)	Ultimate strength (MPa)	Yield plateau $\Delta\varepsilon_y$ (mm)	Ultimate strain ε_u (mm)	Young's Modulus (Mpa)	Poisson's ratio
7850	470	620	0.017	0.11	206000	0.3

The elastic-plastic behavior of the sleeve connector is carried on using a bilinear model without consideration of the hardening strain of steel material. The ultimate stress of the sleeve duct is given as 550 MPa, and the yield considered in this work is set at 450 MPa from [28]. The manufacturer tested the material model of the sleeve iron duct, which is presented in Tab. 2.

Tab. 2 - Material model of the reinforcement bar

Mass (kg/m ³)	Density	Elastic		Plastic
		Young's Modulus (MPa)	Poisson's ratio	Ultimate strength (MPa)
7300		203000	0.3	550

The injected grounding materials achieved an average compressive strength of 89 MPa. The grouting materials are modeled using the Concrete Damaged Plasticity (CDP) model available in Abaqus commercial software modified for concrete under active confinement following Lubliner's model [29]. For better accuracy, the post-failure modeling of grouting materials considers tensile stiffeners to allow residual stress through the crack until total failure. The CDP model for the grouting materials is established based on their empirical, experimental verification for each parameter [30-35]. The adopted CDP parameters in this research are presented in Tab. 3.

Tab. 3 - Grouting material model [30-35]

Parameters	Mass density (kg/m ³)	Elastic		Plastic				
		Elastic modulus Mpa	Poisson's ratio	Dilatation angle Ψ	Eccentricity	f_{bo}/f_{co}	K	Viscosity parameter
Model properties	2500	38000	0.2	38	0.1	1.16	0.66	0.0001

Test specimen and defect distribution

The experiment considered in this study aimed at assessing the amplitude of the bond strength degradation induced by the different locations of the defect and resulting consequences on the tensile performance of the grouted sleeve connector. The preset defects in grouting materials within the grout-bar bonding zone were made of a silicon rubber tape of 2mm thickness tied around the bar in different lengths 1d, 2d, and 3d where d is the diameter of the bar respectively in six different locations for each specimen as illustrated in Fig. 1.

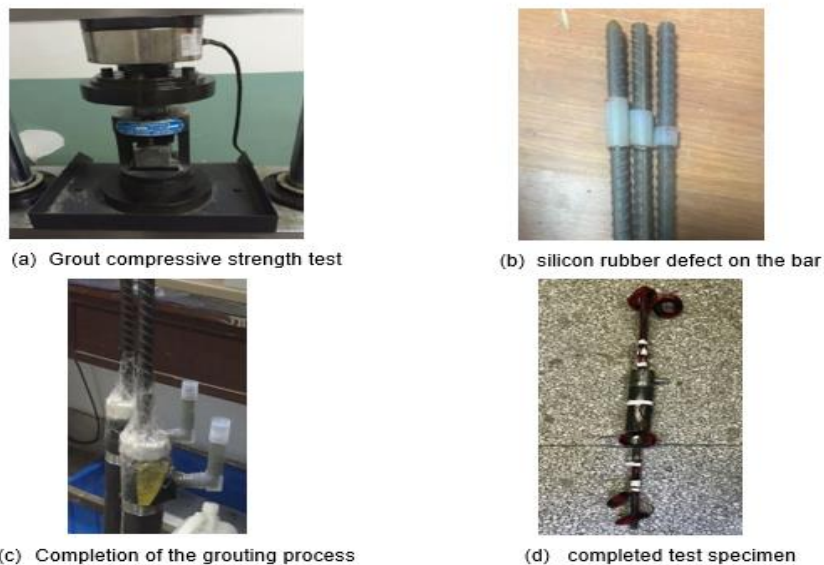


Fig. 1 – overall preparation of the test specimens

A total of 18 test specimens with defects of different sizes were made to test the influence of defects of different sizes in different locations on the tensile performance of the connector. In Fig. 2, the different arrangements of defects in the specimen are presented. The proposed configurations of the defects were based on the probability of occurrence of the defects during

the onsite operations of grouting. The defects are first considered for a single reinforcement and later for both reinforcement bars lapped within the connector, as sketched in Fig. 2.

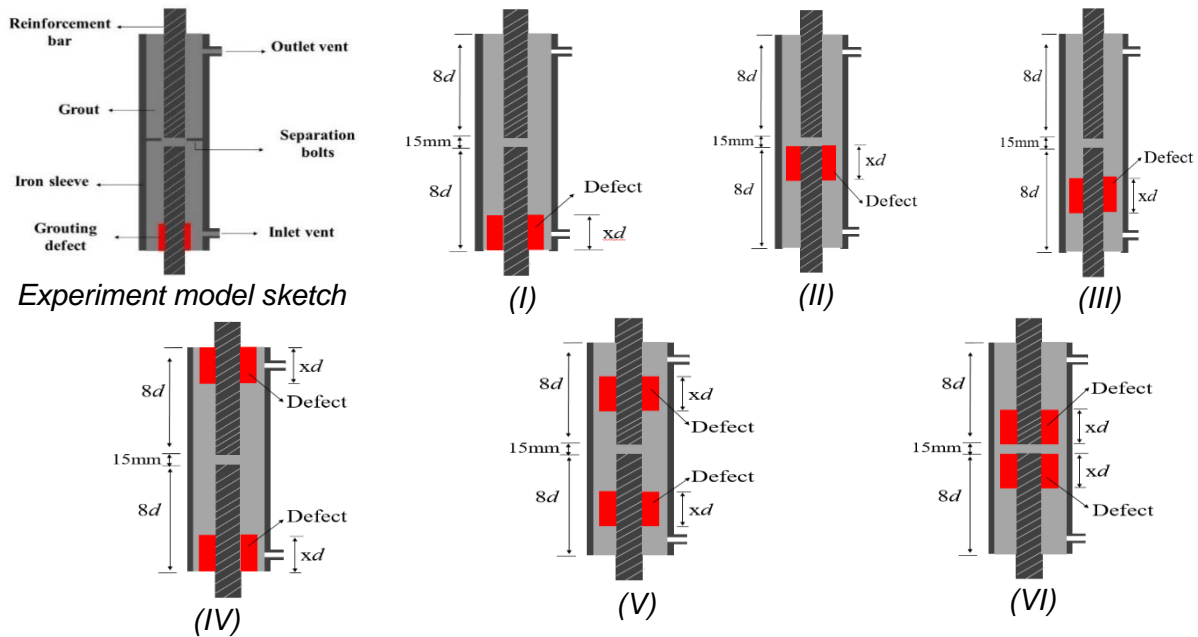


Fig. 2 – overall preparation of the test specimens

The unidirectional static tensile load was applied by the universal hydrostatic tensile loading machine of the maximum capacity of 300KN at a rate of 28KN/min. The loading method based on the JGJ1407-2016 technical regulations for mechanical connections of reinforcement bars with a sleeve and was completed in the following process $0 \rightarrow 0.6 f_{yk}$ (measure residual deformation) \rightarrow max Tensile force (record the tensile strength) $\rightarrow 0$ (determine the total elongation at the maximum force).

Experimental results and discussion

As presented in this work, the tensile experiment of the defective grouted sleeve connector recorded some parameters that inform the analysis of the connector's performance. These parameters include but are not limited to the Yield Force, the Ultimate load, the total elongation and the observed failure mode for each specimen.

The representative Load displacement curves of the experimental results can be portrayed through the specimens of configurations I, II, III, and IV as shown in Fig. 3. To summarize the impact of defects based on their position along the anchorage length of the reinforcement bar.

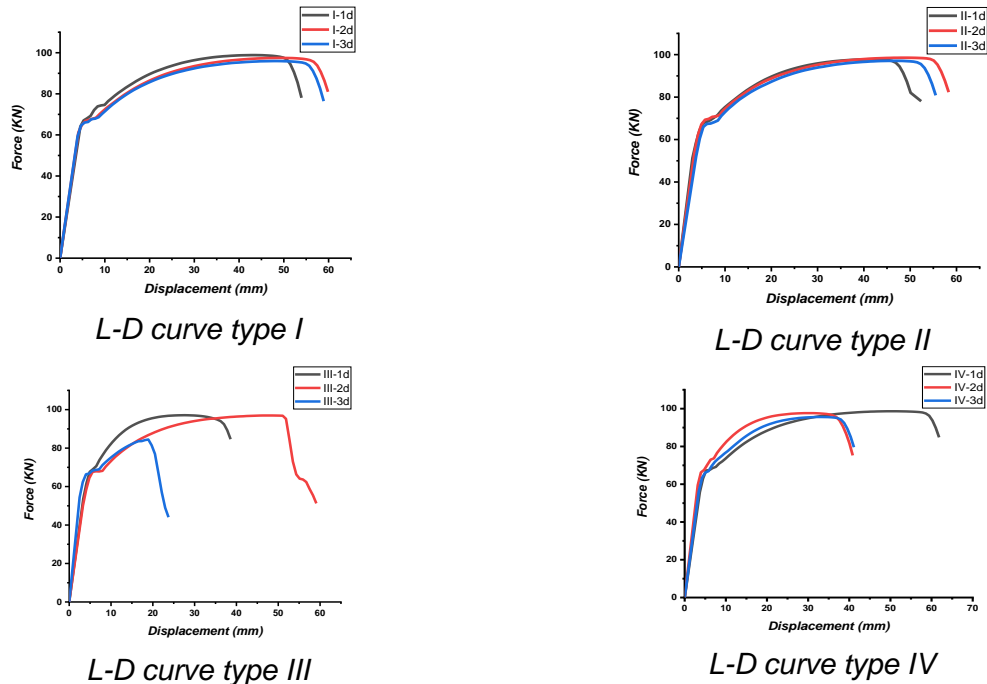


Fig. 3 – Representative L-D plots of tensile test

All specimens considered in this experiment failed in the plastic loading stage of the connector after the yielding point. This reveals that an active anchorage length of the bar of value $\geq 5d$ can enhance the tensile performance of the connector beyond the yielding point regardless of the location of the defect. However, the ultimate tensile capacity of the connection is considerably affected by the location of the defect when the active anchorage length is $5d$. This is further explained by the premature drop of plot III-3d in Fig. 3. Thus, the location of the defect in configuration III threatens the integrity of the connection.

Considering the findings in Fig. 3, the connector's performance shows great sensitivity to the defect location, especially in test specimens where the defect size is $2d$ and $3d$. This indicates that a defect of small size ($1d$) has a minor impact on the connector's performance regardless of the location and much more when the active anchorage length of the bar is $7d$. The impact of the location of the defect is observed when the size of the defect is $2d$ and $3d$. When the defect is of size $3d$ in arrangement III where the defect is located in the mid-span of the bar, the drop in the ultimate capacity and bond strength of the connector is 19.6% . Whereas, when the same defect is preset on both reinforcement bars within the connector, the resulting drop in capacity is approximately 16% . The bond strength of the connector shows a trend of performance recovery when a similar defect is located on both ends of the reinforcement bars in the specimen. The improved performance also observes a decrease in the total elongation. This phenomenon results from the instability due to the unequal distribution of stresses between the two ends of the connector when the defect is located on one side of the reinforcement resulting in structural instabilities due to the deterioration of the bond capacity of the defective side. The location of defects in bonding zones of both ends of the reinforcements promotes an equal and symmetric response of the connector enhanced by the equal bond capacity of a single reinforcement,

enhancing the stability of the connector. Studies in the subsequent section consider how defects interact with the confinement effect to identify the most suitable configuration of the connection and the risk associated with defects.

VALIDATION OF THE NUMERICAL MODEL

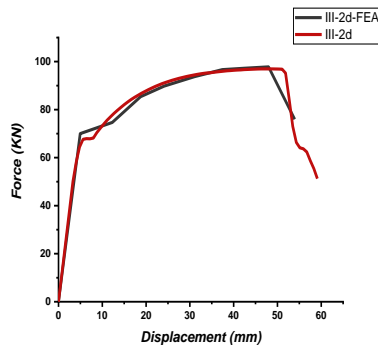
The grout-bar bond constitutes the bonded interface and are modeled in Abaqus using a friction-based interfacial model with contact pressure P . The slip of the bond strength occurs at a critical value of the shear strength τ_{crit} between interfaces and corresponds to the yield value of the actual bond strength.

Model validation

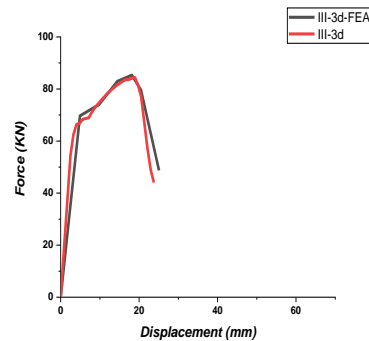
The model's accuracy is established based on its ability to predict the connector's behavior when subjected to similar loading and boundary conditions. The relevant test output of the experiments, including the tensile capacity of the connector and the failure phenomenon, is set as the main indicator to test the model's validity.

Load resistance prediction

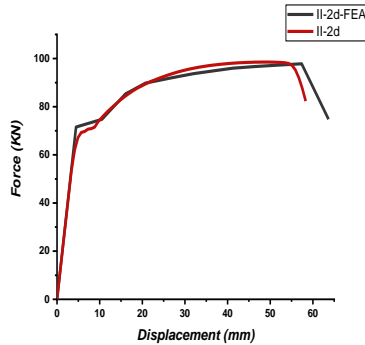
To further validate the performance of the proposed models, the load resistance is an important indicator of the good accuracy of the computational model to simulate the experiment. For this purpose, some selected typical load-displacement curves resulting from the numerical models' computation are plotted on the same chart as those resulting from this work's experiment, as presented in Fig. 4.



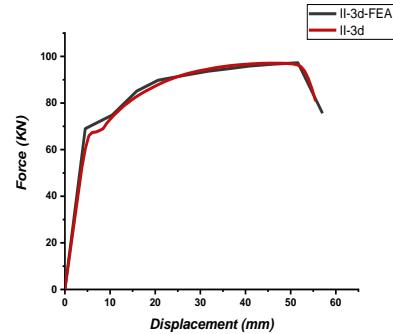
(a) Specimen III-2d L-D comparison



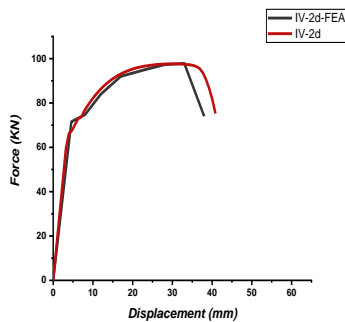
(b) Specimen III-3d L-D comparison



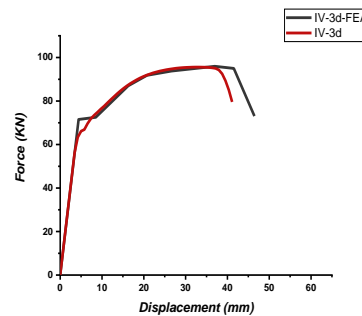
(c) Specimen II-2d L-D comparison



(d) Specimen II-3d L-D comparison



(e) Specimen IV-2d L-D comparison



(f) Specimen II-3d L-D comparison

Fig. 4 – Load resistance prediction

The load resistance of the connector is accurately predicted following the similar trend of the load-displacement curves of both FEA and experimental findings. The main points of the load-displacement curves are also located at almost similar loading magnitude and equivalent displacement, which is proof of the proposed model's reliability to adequately predict the mechanical properties of the grouted sleeve connection.

Failure mode prediction

The proposed model has predicted the connector's behavior with a similar trend of materials performance when subjected to tensile loading. Similar to the experiment, the numerical models captured the connector's sensitivity to the defect's location and its induced consequence on the failure modes. Fig. 5 presents the failure mode prediction by the numerical models.

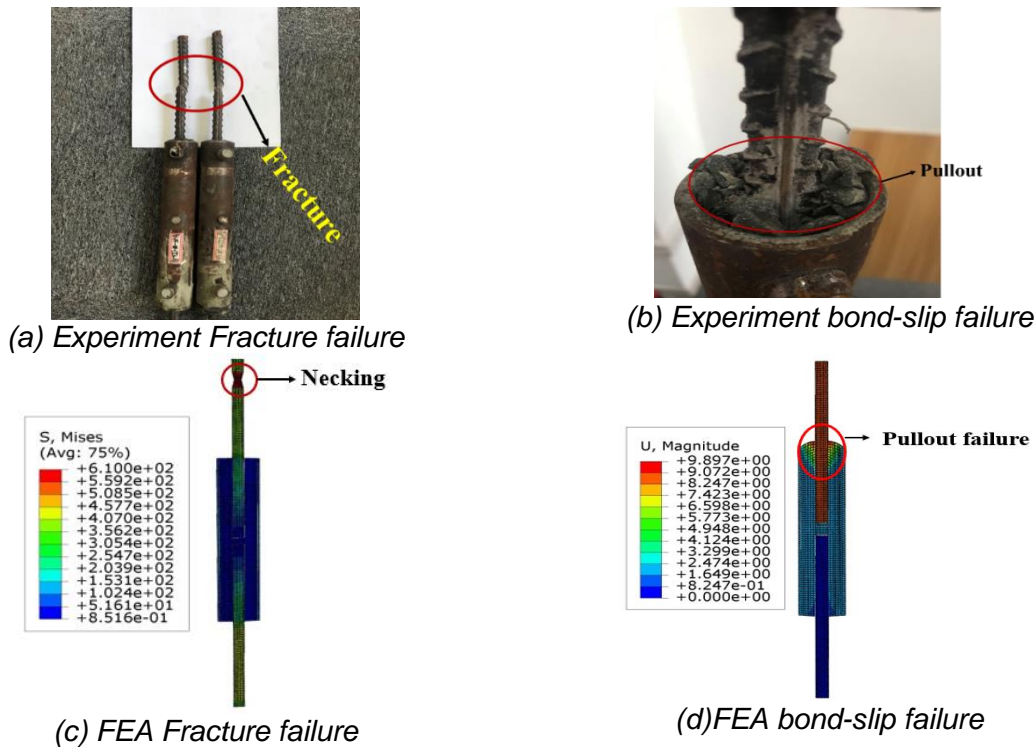


Fig. 5 - Failure mode prediction of the model

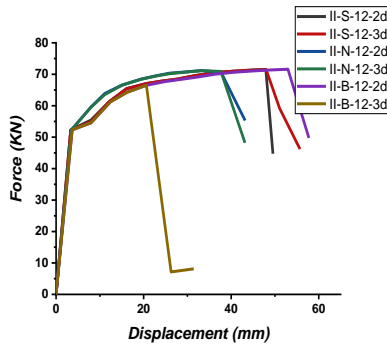
The fracture failure of the connector indicates the ability of the connector to sustain the overall performance of the reinforcement bar or even better. It's achieved by adequate bond resistance to the tensile pull-out forces until the yielding and the reinforcement fracture. The slip failure on the other end indicates the connector's weakened bond performance, which does not sustain the tensile capacity of the bar to its fracture. Through both numerical analysis and experiment, this failure mode is engendered by the defects and their location, which compromises the resistance of the connector by accumulating stresses in one zone. Based on the findings presented in Tab. 1, all the specimens predesigned with defects of size $1d$, and the numerical models with similar defects failed by the fracture of the reinforcement. This indicates that the active bond developed along the anchorage length of $7d$ sustains the connector's tensile capacity regardless of the defect's location. When the length of the defect is $2d$, the specimen with the preset defect in the midspan of one end of the bars in arrangement III experiences a slip failure. The location of the defect in this configuration prompts the slip failure even when the effective anchorage length of the bar is $6d$. The bond strength is considerably compromised when the defect's length is $3d$ and explains most of the pull-out failures. Nevertheless, when the defect is located in both edges of the connector, the influence of the defect of length $3d$ becomes minor when the defect is located in the edges of the connector. Therefore, the parametric analysis will be conducted on arrangements II, III, and IV models.

PARAMETRIC STUDY

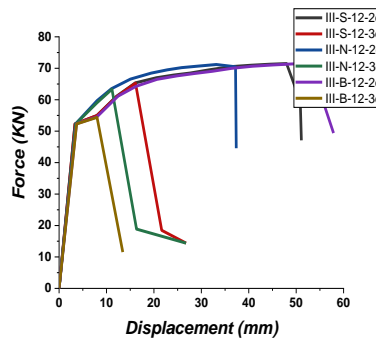
The parametric study proposed in this research evaluates the influence of the confinement effect by changing the ratio of the sleeve diameter to that of the bar (d_s/d) from the lower limit to the upper limit of the design specified values {2.66-3.55} [36]. Three degrees of confinement effects are considered. The one established from the experiment in this work is denoted by N with the ratio value of 3.2. The smallest recommended value of the ratio denoted by S has the value of $d_s/d=2.66$, and the biggest allowable value, the ratio $d_s/d=3.55$, is denoted as B. Three diameters of the reinforcement bar, 12, 14, and 16mm, are considered in this parametric. Specimens are labeled based on their configuration (arrangement), the diameter of the bar, d_s/d ratio index, and the size of the defect in the following sequence configuration-bar-diameter-confinement index-length of defect i.e. II-16-N-2d.

Effect of the degree of confinement on the load-resistance of the connector

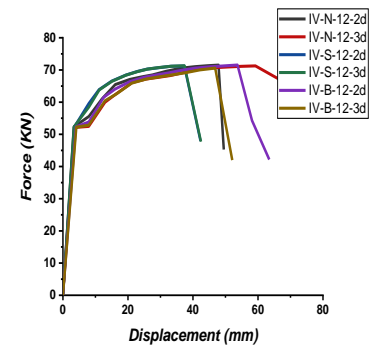
The evaluation of the impact of the confinement effect on the load-bearing capacity of the connection can be assessed by comparing the plots when the diameter of the connector varies for each of the three types of configurations in consideration with different degrees of confinement S, N, and B. The plots in Fig. 6 summarize the behavior of the Load-displacement curves of the connector in different types of configurations.



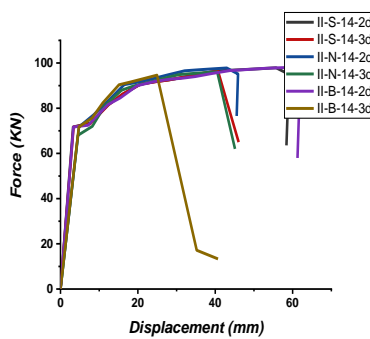
(a) L-D curves for type II-12



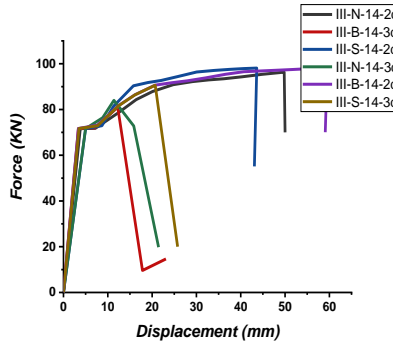
(b) L-D curves for type III-12



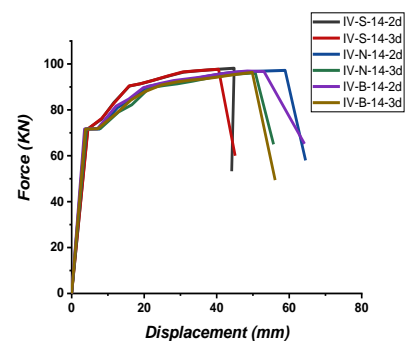
(c) L-D curves for type IV-12



(d) L-D curves for type II-14



(e) L-D curves for type III-14



(f) L-D curves for type IV-14

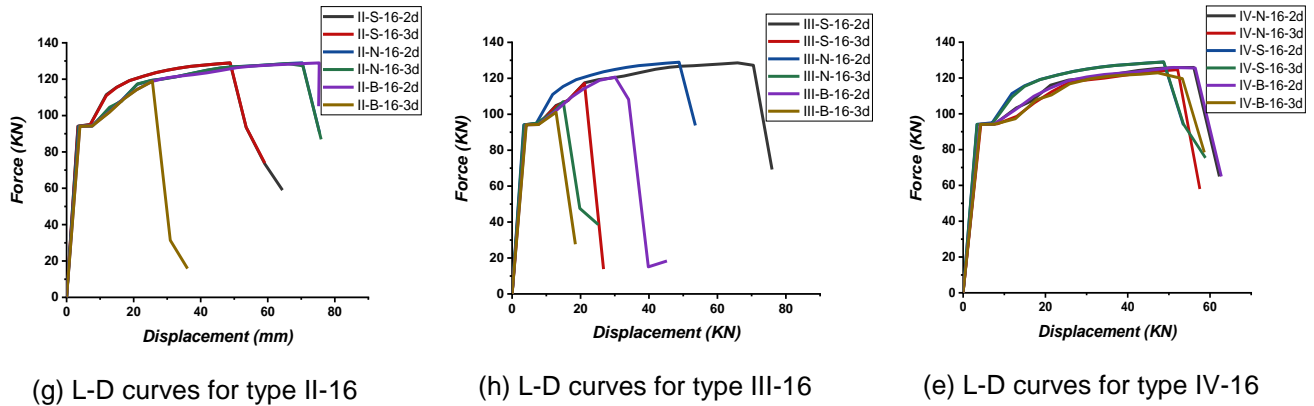


Fig. 6 – Load displacement of the connector for different degrees of confinement

The influence of the confinement effect based on the d_s/d ratio is analyzed in combination with the changes of the reinforcement diameter in the configuration of three types of defects as presented earlier. In inference to the outputs presented in Fig. 6, the connectors response presents trends influenced by the location of defects, size of the defects, and the confinement effect, whereas the effect of the diameter of the reinforcement is limited in changing the tensile capacity of the connector but has negligible influence on the trend of the load-displacement response of the connector.

The peak value of the bond performance is registered at the lowest value of the d_s/d ratio in all plots. This is due to the sleeve's smaller diameter, which enables a higher impact of the lateral pressures in the effective bonding zone where the resistance of the connector is formulated. The largest value of the ratio experiences the lowest bond resistance as a result of the decreased impact of the confining pressures in the bonding zone. Nevertheless, the significance and impact of the confinement effect on the bond strength shrink as the performance of the connector regains the strength from the smaller size of the defect. Thus, the effect of confinement may be negligible when the bond strength is sustained by an adequate anchorage length of the bar in a normal configuration.

Impact of defects on the stress distribution within the connector

The main way defects can compromise the connector's performance is by changing the distribution of stresses through the components of the connector. The proposed numerical model in this study has sensibly tracked the influence of the location of the defects on the distribution of stresses among the components of the connector. Fig. 7 presents the influence of defects on the distribution of stresses to each part of the connector and the resulting impact on the overall tensile performance of the connector.

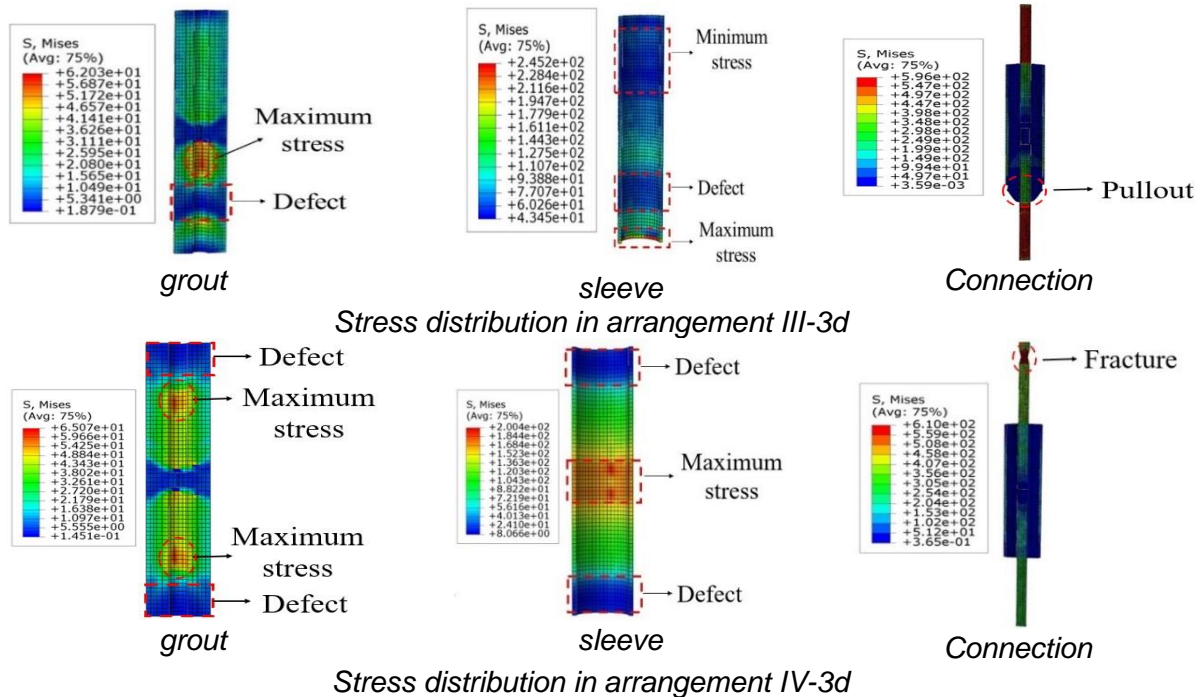


Fig. 7– Influence of the defect location on the distribution of stresses

Arrangement III provides the sensitive location of the defect. In contrast, arrangement IV enhances the asymmetric distribution of stresses within the connector and improves the connector's performance due to the stability and symmetric loading enhanced in either side of the reinforcement.

Effect of the confinement effect on the failure mode

One of the main influences of the different degrees of confinement on the mechanical performance of the grouted sleeve connection is the modification of the failure mechanisms from slip to fracture and vice-versa. In specimens with the sensitive location of the defects, the premature slip failure can result from a significant drop in the ultimate load-bearing capacity of the connection when subjected to tensile loading. Tab. 4 presents the specimens which registered a change in the failure mechanism from their initial failure modes due to the effect of confinement based on the d_s/d ratio.

Tab. 4 - Change of failure mechanism under different confinement effects

Model label	Initial failure mode (N)	New failure mode	d_s/d ratio
II-S-12-3d	Slip out	Fracture	S
II-B-12-2d	Fracture	Slip out	B
III-S-12-2d	Slip out	Fracture	S

IV-B-12-3d	Fracture	Slip out	B
II-S-14-3d	Slip out	Fracture	S
II-B-14-2d	Fracture	Slip out	B
III-S-14-2d	Slip out	Fracture	S
IV-B-14-3d	Fracture	Slip out	B
II-S-16-3d	Slip out	Fracture	S
II-B-16-2d	Fracture	Slip out	B
III-S-16-2d	Slip out	Fracture	S
IV-B-16-3d	Fracture	Slip out	B
IV-B-16-2d	Fracture	Slip out	B

Inferring from the data in Tab. 4 models change from the slip failure in the N ratio index specimens to the fracture failure due to a small value of the ds/d ratio, which increases the impact of confinement pressures in the effective bond zone and consequently improves the tensile resistance of the connector leading to the fracture of the reinforcement bar. The contrast of this mechanism is observed within the specimen, which switched from a fracture failure in normal configurations to a pull-out failure in a specimen with a higher value of the ds/d ratio. This aspect is due to the dissipation of the confinement forces in the big layer of grouting materials hence reaching the effective bonding zone with a small magnitude resulting in the slip of the bar due to the declining bond strength compared to the specimen in which the lateral pressures traverse a relatively thin layer of grouting materials and attain the effective bond zone with a higher magnitude. The effect of confinement is empirically reported in related studies to impact the nature of concrete/bar bonds. A similar observation result from the parametric study of the defective grouted sleeve in this work is significant.

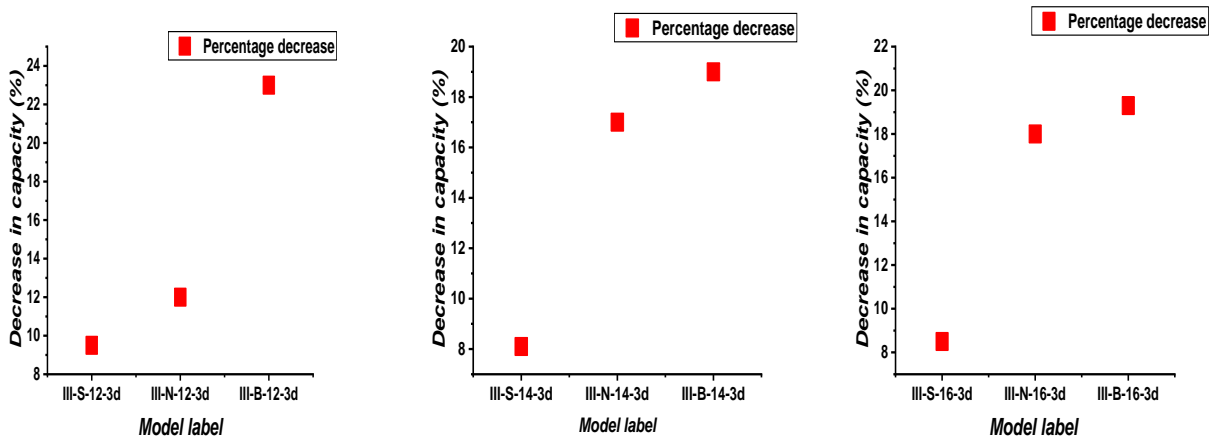
The change in the failure mechanism of the connector due to the confinement effects is not affected by the diameter of the reinforcement bar but rather the location of the defect and its size. Therefore, regardless of the diameter of the bar, similar configurations of the models registered an identical impact of the confinement effects on the switch of their failure mechanism. This aspect tends to limit the influential parameters of the mechanical properties of the grouted sleeve connector to the confinement effect, the location, and the size of the defects.

Influence of the confinement effect on the ultimate capacity of the connector

Another impact of the different degrees of confinement on the mechanical performance of the connector is observed in a significant change in the ultimate tensile capacity of the connector when subjected to loading. A significant loss in tensile capacity of the connector was reported in specimen with configurations II as a result of the decrease in the degree of confinement due to the enlargement of the diameters' ratio to the index B. When the defect length is $3d$, in all specimens of type (III-3d), regardless of the confining effect, there was a loss in the capacity due to the nature of defects though at different rates as a result of degrees of confinement

In Fig. 8, the highest percentage decrease in the ultimate capacity is 9.8 observed when the diameter of the reinforcement is 12. While keeping a similar configuration, an increase in the diameter of the bar decreases the rate at which the ultimate capacity of the connector drops.

Therefore, the biggest diameter of the bar has the smallest value of the percentage of decrease in ultimate capacity. In respect to this scenario, the bond strength of the larger diameter of the bar deteriorates slower when the confinement pressure decreases.



Capacity decrease in III-12-3d Capacity decrease in III-14-3d Capacity decrease in III-16-3d

Fig. 8 – Percentage drop in ultimate capacity due to increased ratio in III-3d configuration

The decrease in the capacity due to the different degrees of confinement in a specimen of configuration III, when the length of defect is 3d, registers a recovery when the ratio is at the smallest value of 2.66, as presented in Fig. 8. The percentage of decrease in capacity is around between 8-10 when the ds/d ratio is in a small range (S) for all reinforcement diameters. In contrast, the biggest ratio leads to the highest percentage of decrease in the ultimate tensile capacity of the connector. The smallest diameter of the reinforcement appears to be more susceptible to the decrease in the confinement pressure of the connector and experiences the highest value of the percentage decrease in the tensile capacity of the connector. In contrast, the enlargement of the diameter of the bar slows down the influence of the decreased confinement pressures. The explanation of this scenario is not straightforward; however, the larger diameter of the bar generates a large bonding zone compared to a small value of the diameter. The contribution of the confinement effect may be therefore decreasing with the enlargement of the bar diameter as well.

Since the embedded length of the connector 5d can sustain the Performance of ultimate Performance of the connector up to fracture in some specimens and yet exhibits a premature failure in other specimens due to the location of the defect, there is a need to modify the bond strength calculation in the structural health monitoring when the effective embedded length is 5d. Considering the changes in the capacity resulting from the connector due to the confinement effects in the design ranges of the ratio ds/d, the equation for the average bond strength, which considers the ultimate load needs to be modified for design optimization when the defects are detected within the connector.

The initial bond strength equation

$$\mu = \frac{F}{\pi d l_e} \quad (1)$$

F is the ultimate applied load, d is the diameter of the bar and l_e is the anchorage length of the reinforcement. For the ultimate state design of the bond resistance of grouted sleeve connection, the effect of confinement effect and the location of the defect when the anchorage length is 5d should be considered in the modified expression for the average bond calculation. The constant of safety design accounting for the confinement pressure and the defect is f'_c . The modified equation for the average bond calculation can be written as

$$\mu' = f'_c \frac{F}{\pi d l_e} \quad (2)$$

The safety constant $f'_c = 0.92$ when the ds/d ratio index is S (2.66) and $f'_c = 0.77$ when the ds/d ratio index is B (3.55).

CONCLUSIONS

This paper analyzes the influence of the degrees of confinements in the allowable interval of the ratio of the sleeve diameter to the diameter of the bar on the bond strength and tensile capacity of the grouted sleeve connector predesigned with defects. This article presents the experimental program subjecting the connector with predesigned defects in different locations to the tensile test, validating the proposed numerical models, and conducting a parametric analysis with the three main degrees of confinements based on the diameters' ratio. The following conclusions are derived.

The grouted sleeve connection is sensitive to the location of the defects, which determines if the defects present a high risk, mild risk, and minor risk to the structural integrity of the connection.

The presence of defects in the connector influences its performance by creating overstressed zones within the connector due to the interruption in the normal symmetric and equal distribution of loading stresses resulting in the early failure in some specimens.

The effect of confinement considerably influences the connector's failure mechanism regardless of the bar's diameter. The lower ratio value switches the failure modes of some specimens from pull-out to fracture, while its value in the upper limits of the ratio's interval engenders the opposite phenomenon.

The lowest recommended value of the diameters' ratio considerably improves the bond strength and results in approximately 10% to 16% recovery of the decreased tensile performance due to defects in the high-risk zone and a low degree of confinement.

For an optimized limit state design, the average bond strength can be improved by a safety constant (f'_c), which incorporates the impact of the defects' location and the effect of confinement on the bond strength of the connector.

The significance and impact of the confinement effect on the performance of the connector shrink become negligible when the bond strength is sustained by an adequate anchorage length of the bar in a normal configuration.

ACKNOWLEDGEMENTS

The study presented in this paper was supported by China's National Natural Science Foundation (Grant No. 51608234) and the Natural Science Foundation of Jiangsu Province of China (Grant No. BK20160534), which are gratefully acknowledged.

REFERENCES

- [1] Martin, L.D. and C.J. Perry, *PCI design handbook: precast and prestressed concrete*. 2004: Prestressed Concrete Inst.
- [2] Lu, Z., et al., *Mechanical behaviour of grouted sleeve splice under uniaxial tensile loading*. Engineering Structures, 2019. **186**: p. 421-435.
- [3] Qiong, Y. and X. Zhiyuan, *Experimental study of grouted sleeve lapping connector under tensile load*. Građevinar, 2017. **69**(06.): p. 453-465.
- [4] Yuan, H., et al., *Tensile behavior of half grouted sleeve connections: Experimental study and analytical modeling*. Construction and Building Materials, 2017. **152**: p. 96-104.
- [5] Liu, Y.J., C. Li, and W.J. Zhou. *Numerical analysis on tensile properties of grout-filled splice sleeve rebars under ISO 834 standard fire*. in *E3S Web of Conferences*. 2018. EDP Sciences.
- [6] Ameli, M., et al., *Seismic column-to-footing connections using grouted splice sleeves*. ACI Structural Journal, 2016. **113**(5): p. 1021.
- [7] Ameli, M. and C.P. Pantelides, *Seismic analysis of precast concrete bridge columns connected with grouted splice sleeve connectors*. Journal of Structural Engineering, 2017. **143**(2): p. 04016176.
- [8] Haber, Z.B., M.S. Saiidi, and D.H. Sanders, *Seismic Performance of precast columns with mechanically spliced column-footing connections*. ACI Structural Journal, 2014. **111**(3): p. 639-650.
- [9] Qu, H., et al., *Investigation and verification on seismic behavior of precast concrete frame piers used in real bridge structures: Experimental and numerical study*. Engineering Structures, 2018. **154**: p. 1-9.
- [10] Zheng, Y., et al., *Performance and confining mechanism of grouted deformed pipe splice under tensile load*. Advances in Structural Engineering, 2016. **19**(1): p. 86-103.
- [11] Dancygier, A.N., A. Katz, and U. Wexler, *Bond between deformed reinforcement and normal and high-strength concrete with and without fibers*. Materials and Structures, 2010. **43**(6): p. 839-856.
- [12] Hosseini, S.J.A., *Bond Behaviour of Grouted Spiral and Splice Connection Under Direct Axial and Flexural Pullout Load*. 2015, Universiti Teknologi Malaysia.
- [13] Lee, J.-Y., et al., *Bond behaviour of GFRP bars in high-strength concrete: bar diameter effect*. Magazine of Concrete Research, 2017. **69**(11): p. 541-554.
- [14] Sayadi, A.A., et al., *The relationship between interlocking mechanism and bond strength in elastic and inelastic segment of splice sleeve*. Construction and Building Materials, 2014. **55**: p. 227-237.
- [15] Rolland, A., et al., *Analytical and numerical modeling of the bond behavior between FRP reinforcing bars and concrete*. Construction and Building Materials, 2020. **231**: p. 117160.
- [16] Kim, H.-K., *Bond strength of mortar-filled steel pipe splices reflecting confining effect*. Journal of Asian Architecture and Building Engineering, 2012. **11**(1): p. 125-132.
- [17] Xing, G., et al., *Experimental study on bond behavior between plain reinforcing bars and concrete*. Advances in Materials Science and Engineering, 2015. **2015**.
- [18] Jiang, T., et al., *Three-dimensional nonlinear finite element modeling for bond performance of ribbed steel bars in concrete under lateral tensions*. International Journal of Civil Engineering, 2020: p. 1-23.
- [19] Xu, F., et al., *Experimental bond behavior of deformed rebars in half-grouted sleeve connections with insufficient grouting defect*. Construction and Building Materials, 2018. **185**: p. 264-274.
- [20] Zheng, G., et al., *Mechanical Performance for defective and repaired grouted sleeve connections under uniaxial and cyclic loadings*. Construction and Building Materials, 2020. **233**: p. 117233.
- [21] Zhang, W., et al., *Experimental study on post-fire performance of half grouted sleeve connection with construction defect*. Construction and Building Materials, 2020. **244**: p. 118165.
- [22] Hosseini, S.J.A. and A.B.A. Rahman, *Effects of spiral confinement to the bond behavior of deformed reinforcement bars subjected to axial tension*. Engineering Structures, 2016. **112**: p. 1-13.
- [23] Torre-Casanova, A., et al., *Confinement effects on the steel-concrete bond strength and pull-out failure*. Engineering Fracture Mechanics, 2013. **97**: p. 92-104.

- [24] Wang, Z., et al., *Experimental study on a novel UHPC grout-filled pipe sleeve with mechanical interlocking for large-diameter deformed bars*. Engineering Structures, 2021. **226**: p. 111358.
- [25] Berra, M., et al., *Steel-concrete bond deterioration due to corrosion: finite-element analysis for different confinement levels*. Magazine of Concrete Research, 2003. **55**(3): p. 237-247.
- [26] Espoir, K.K., X. Fuzhe, and G. Haojie, *GROUTED SLEEVE CONNECTION FOR PRECAST CONCRETE MEMBERS*. Civil Engineering Journal, 2020. **28**(4).
- [27] Kahama, E.K., X. Fuzhe, and D.-L. M. Anglaaere, *Numerical study on the influence of defects in grouting on the mechanical properties of a full grouted sleeve connector*. The Journal of Adhesion, 2021: p. 1-32.
- [28] Guo, H., J. Zhang, and C. Wang, *Experimental Study on Influence of Connection Defects on Joint Strength of Half-Grouted Sleeve Splicing of Rebar*. Advances in Civil Engineering, 2020. **2020**.
- [29] Lubliner, J., et al., *A plastic-damage model for concrete*. International Journal of solids and structures, 1989. **25**(3): p. 299-326.
- [30] Hany, N.F., E.G. Hantouche, and M.H. Harajli, *Finite element modeling of FRP-confined concrete using modified concrete damaged plasticity*. Engineering Structures, 2016. **125**: p. 1-14.
- [31] Kmiecik, P. and M. Kamiński, *Modelling of reinforced concrete structures and composite structures with concrete strength degradation taken into consideration*. Archives of civil and mechanical engineering, 2011. **11**(3): p. 623-636.
- [32] Manual, A.S.U.s., *Abaqus 6.11*. <http://130.149>, 2012. **89**(2080): p. v6.
- [33] Ma, Y.-X., O. Zhao, and K.H. Tan, *Experimental and numerical studies of concrete-encased concrete-filled steel tube stub columns under uniaxial and biaxial eccentric compression*. Engineering Structures, 2021. **232**: p. 111796.
- [34] Ren, W., et al., *Numerical simulation of prestressed precast concrete bridge deck panels using damage plasticity model*. International Journal of Concrete Structures and Materials, 2015. **9**(1): p. 45-54.
- [35] Raza, A., et al. *Finite element modelling and theoretical predictions of FRP-reinforced concrete columns confined with various FRP-tubes*. in *Structures*. 2020. Elsevier.
- [36] Brenes, F.J., S.L. Wood, and M.E. Kreger, *Anchorage requirements for grouted vertical-duct connectors in precast bent cap systems*. 2006.